Observational Study

Medicine®

OPEN

Percentage change of primary tumor on ^{18}F-FDG PET/CT as a prognostic factor for invasive ductal breast cancer with axillary lymph node metastasis

Comparison with MRI

Jang Yoo, MD[a,b], Bom Sahn Kim, MD, PhD[a,*], Jin Chung, MD, PhD[c], Hai-Jeon Yoon, MD[a]

Abstract

We evaluated the prognostic value of quantitative parameters using dual time point (DTP) ^{18}F-FDG PET/CT (PET/CT) in invasive ductal breast cancer (IDC) with metastatic axillary lymph nodes (ALN) as compared with dynamic contrast-enhanced (DCE) and diffusion-weighted (DW) MRI.

Seventy patients with IDC and metastatic ALN were retrospectively registered. Static PET parameters including maximum standardized uptake value (SUV_{max}), metabolic tumor volume (MTV), total lesion glycolysis (TLG) of primary tumor, SUV_{max} of ALN (SUV_{ALN}), and percentage changes (Δ%) in those parameters were measured with DTP PET/CT. From DCE MRI, peak enhancement value, total tumor angio volume, and proportions of kinetic curve types on delayed-phases were investigated. The average apparent diffusion coefficient (ADC_{avg}) was estimated on DWI. To demonstrate the prognostic value of quantitative imaging parameters for recurrence-free survival (RFS), univariate and multivariate analyses were performed using those parameters and clinicohistologic variables.

All static PET parameters, $\%\Delta SUV_{max}$, $\%\Delta MTV$, and $\%\Delta SUV_{ALN}$ on DTP PET/CT and ADC_{avg} on DWI were significantly predictive for disease recurrence. Of clinicohistologic variables, pathologic tumor (pT) diameter, pathologic ALN stage, tumor grade, and hormonal status also were significantly prognostic. After multivariate analysis, $\%\Delta SUV_{max} > 25.05$ ($P = .043$), $ADC_{avg} \leq 1016.55$ ($P = .020$), pT diameter > 3 cm ($P = .001$), and ER negative status ($P = .002$) were independent prognostic factors for poor outcome.

Only $\%\Delta SUV_{max}$ of the primary tumor on PET/CT together with ADC_{avg}, pT diameter, and ER status was an independent prognostic factor for predicting relapse in IDC with metastatic ALN. Percentage change of primary tumor on preoperative PET/CT may be a valuable imaging marker for selecting IDC patients that require adjunct treatment to prevent relapse.

Abbreviations: ^{18}F-FDG PET/CT = ^{18}F-fluorodeoxyglucose positron emission tomography/computed tomography, ADC_{avg} = average apparent diffusion coefficient, ALND = axillary lymph node dissection, ANL = axillary lymph node, BCS = breast conserving surgery, CI = confidence interval, DCE-MRI = dynamic contrast-enhanced magnetic resonance imaging, DTP = dual time point, DWI = diffusion-weighted imaging, ER = estrogen receptor, HER2 = human epidermal growth factor receptor 2, IDC = invasive ductal breast cancer, MRM = modified radical mastectomy, MTV = metabolic tumor volume, pN = pathologic lymph node, PR = progesterone receptor, pT = pathologic tumor, RFS = recurrence-free survival, ROC = receiver-operating characteristic, ROI = region of interest, SD = standard deviation, SUV_{max} = maximum standardized uptake value, TLG = total lesion glycolysis.

Keywords: diffusion weighted imaging, dual time point ^{18}F-FDG PET/CT, dynamic contrast, invasive ductal breast cancer, magnetic resonance imaging, recurrence-free survival

Editor: Saad Zakko.

The scientific guarantor of this publication is BSK. The authors of this study declare no relationships with any companies whose products or services may be related to the subject matter of the article. This research was supported by grants from the National Research Foundation (2015R1C1A1A02037051, 2012M3A9B6055379) of South Korea. Institutional Review Board approval was obtained and written informed consent was waived.

The authors declare no conflict of interest.

[a] Department of Nuclear Medicine, Ewha Womans University School of Medicine, [b] Sungkyunkwan University School of Medicine, [c] Department of Radiology, Ewha Womans University, School of Medicine, Seoul, South Korea.

[*] Correspondence: Bom Sahn Kim, Department of Nuclear Medicine, Ewha Womans University School of Medicine, Seoul, South Korea (e-mail: kbomsahn@ewha.ac.kr).

Medicine (2017) 96:31(e7657)

Received: 20 April 2017 / Received in final form: 27 June 2017 / Accepted: 11 July 2017

http://dx.doi.org/10.1097/MD.0000000000007657

1. Introduction

^{18}F-fluorodeoxyglucose (FDG) positron emission tomography/computed tomography (PET/CT) has been used to detect enhanced cancer cell glycolysis and identify malignant lesions, stage work-up, determine disease recurrence, and monitor treatment response in various oncologic settings, including breast cancer. FDG is transported by glucose transporters, metabolized by the enzyme hexokinase and builds up in cancer cells. FDG uptake within cells mainly depends on cellular metabolic activity and the number of glucose transporters. However, this mechanism is not specific to cancer cells. FDG can accumulate in inflammatory cells and benign processes, causing false-positive findings.[1,2] Recently, several studies have been conducted to overcome these limitations using dual time-point (DTP) PET/CT.[3,4] It is widely assumed that continuous increasing FDG uptake over time after intravenous administration indicates malignancy, whereas a decreasing or stable tendency for FDG affinity indicates inflammation or benign processes. This assumption can also be applied to DTP PET/CT, not only to improve diagnostic performance, but also determine the degree of aggressiveness in breast cancer.

Another imaging modality, magnetic resonance imaging (MRI) is being increasingly performed for breast cancer diagnosis. Dynamic contrast enhanced MRI (DCE-MRI) can increase accuracy for differentiating breast cancer from normal tissue by assessing morphologic characteristics and quantitative kinetic profiles of breast lesions.[5,6] Diffusion-weighted imaging (DWI) can measure the mobility of water molecules in biologic tissues and represent the microscopic cellular environment, and provide additional information such as biophysical features complementary to DCE-MRI.[7] These advanced MRI techniques play clinically important roles in the identification of malignant lesions and determination of disease prognosis and treatment response.[8,9]

There are many clinicohistologic prognostic factors in breast cancer patients. Among these factors, axillary lymph node (ALN) status is highly associated with disease prognosis and has been demonstrated to be the most significant prognostic factor in previous studies.[10,11] The next logical step is identification of prognostic factors in ALN-positive breast cancer to identify high-risk subpopulations that could benefit from adapted treatment and follow-up plans. To the best of our knowledge, no previous studies have investigated the prognostic value of imaging parameters using DTP PET/CT, DCE-MRI, and DWI, simultaneously.

The purpose of this study was to demonstrate prognostic factors by comparing each imaging parameter derived from DTP PET/CT, DCE-MRI, and DWI and clinicohistologic variables for recurrence-free survival (RFS) in invasive ductal breast carcinoma (IDC) with metastatic ALN.

2. Methods

2.1. Patients

A retrospective review of our hospital database between November 2010 and April 2014 identified 230 eligible patients who were diagnosed with IDC and underwent preoperative DTP PET/CT, DCE-MRI, and DWI for initial staging workup. The mean time interval between DTP PET/CT and the 2 MRI modalities was 0.2 ± 1.7 days. From the eligible patients, we excluded those who had a previous history of any other malignancy, neoadjuvant chemotherapy or radiotherapy before those imaging modalities, follow-up less than 6 months, or bilateral breast cancer. We also excluded cases that had either pathologic tumor diameters smaller than 1 cm based on the full-width-at-half-maximum of PET[12,13] or were negative for pathologic ALN metastasis. Ultimately, we enrolled 70 patients (mean age 50.5 ± 10.0 years; range, 31–77 years) pathologically confirmed to have metastatic ALN.

This clinical information review was approved by the institutional review board of our hospital and the requirement for informed patient consent was waived because of the retrospective design.

2.2. Treatment and clinical follow-up

In all patients, breast conserving surgery (BCS) or modified radical mastectomy (MRM) with axillary lymph node dissection (ALND) was done according to tumor size and location, results of the sentinel lymph node biopsy, and the corresponding physician's discretion. Systemic chemotherapy was prescribed with a combined regimen containing doxorubicin and cyclophosphamide, adding either paclitaxel or docetaxel, followed by radiotherapy when the necessity arose. After that, hormonal therapy was given to patients depending on individual age and hormonal status. Patients with human epidermal growth factor receptor 2 (HER2) overexpressing breast cancer were treated with trastuzumab with one or more chemotherapy regimens.

During the follow-up period, patients were asked to visit our hospital for regular examinations every 3 to 6 months in the first 2 years and every 6 to 12 months after that. When recurrence was suspected based on clinical symptoms, physical examination and/or imaging studies, additional procedures for pathologic confirmation or relevant imaging modalities (e.g., chest CT, abdomen CT, brain MRI, etc) were performed. RFS was measured from the date of initial diagnosis to the date of the objective result suggesting disease recurrence.

2.3. Clinicohistologic analysis

Clinicohistologic variables, including age, pathologic tumor (pT) diameter, pathologic ALN stage, Black's nuclear grade, and Bloom-Richardson's histologic grade were analyzed. Immunohistochemistry was also evaluated by a direct immunoperoxidase method with antibodies against estrogen receptor (ER), progesterone receptor (PR), and HER2 according to the Allred system and American Society of Clinical Oncology/College of American Pathologists guidelines.[14,15] ER and PR positivity were defined using both scoring parameters of the percentage of positive cells (from 0 to 5) and staining intensity (from 0 to 3). A total score of 0–2 was considered negative for each hormone; 3–8 was considered positive. For HER2 positivity, tumor cells with more than 10% staining were regarded as positive, and those having less than 10% were regarded as negative. For the marker Ki67, overexpression was defined as more than 14% of tumor cells in this study.[16,17]

2.4. Dual time point ^{18}F-FDG PET/CT acquisition protocol

All patients fasted at least 6 hours before intravenous injection of 5.18 MBq/kg (0.14 mci/kg), and fasting serum glucose levels <140 mg/dL were required to proceed. Patients were asked to rest for 1 hour before image acquisition using a Siemens Biograph mCT with 128-slice CT (Siemens Medical Solutions, Knoxville, TN). Before PET scanning, a low-dose CT scan was obtained

without contrast enhancement from the skull base to the proximal thigh in the supine position for attenuation correction. To obtain PET image parameters, an emission scan of 5 to 7 bed positions with 2 minutes per bed position and a maximum spatial resolution of 2.0 mm were also acquired. PET images were reconstructed with 200×200 matrices with an ordered-subset expectation maximum iterative reconstruction algorithm (21 subsets, 2 iterations), a Gaussian filter of 5.0 mm, and a slice thickness of 3.0 mm. Approximately 2 hours after administration of 18F-FDG (mean, 56.8 ± 5.8 minutes; range, 48–71 minutes), delayed-phase imaging was obtained only in the chest region in the same supine position as the earlier scan. Patients were asked to remain in a resting position on the bed to minimize FDG uptake by muscles during both early- and delayed-phase PET/CT acquisition.

2.5. PET/CT image analysis

PET/CT images were interpreted by two experienced nuclear physicians (JY and BSK with 5 years and 13 years of experience, respectively) who were unaware of the clinical information. To assess semiquantitative PET/CT parameters, regions of interest (ROI) were placed over the primary breast tumor and ALN using the automated delineation feature in commercial software (Syngo.via, Siemens Medical Solutions). The maximal standardized uptake value (SUV_{max}), which represents the highest FDG avidity within the ROI of a tumor lesion, was corrected with the individual patient body weight. Metabolic tumor volume (MTV) was measured based on spherical-shaped delineation of a three-dimensional volume of interest (VOI) covering the primary tumor with an isocontour threshold of 40% of the SUV_{max}, as reported previously.[18] Total lesion glycolysis (TLG) was estimated by multiplying MTV by average SUV within the VOIs of the tumor lesion. ROIs were drawn over the area of maximal FDG avidity of ALN to measure the SUV_{max} of ALN (SUV_{ALN}).

These semiquantitative parameters were also obtained from delayed-phase images using the same techniques as with early-phase images. The percentage change of each parameter over interval time was calculated by subtracting the early measurement from the delayed and dividing by the early, as follows: Percentage change (%Δ) = (delayed parameter – early parameter)/early parameter × 100.

2.6. DCE-MRI and DWI acquisition protocol

MRI was performed with a 3.0-Tesla (T) Achieva system (Philips Medical System, Best, the Netherlands) using a bilateral dedicated seven-channel SENSE breast coil in the prone position. An axial, fat-suppressed, fast-echo T2-weighted image was acquired in advance (TR/TE, 5521/70; flip angle, 90 degrees; field of view, 320 mm; matrix, 332/261; slice thickness, 3 mm with no gap; bandwidth, 289 Hz; time acquisition, 4 minutes 23 seconds). Thereafter, axial DWI with single-shot echo planar imaging (b = 0 and 1000 s/mm^2; TR/TE, 6984/78; field of view, 360 mm; matrix, 128/128; number of excitations, 2; slice thickness 4 mm with a 1-mm slice gap; acquisition time, 1 minutes 30 seconds) and pre- and postcontrast axial and sagittal three-dimensional T1-weighted gradient echo with fat saturation sequences were obtained. DWI was obtained along each of the *x*-, *y*-, and *z*-axes. Gadolinium (0.1 mmol/kg body weight of Gd-DTPA; Gadovist, Bayer Schering Pharma AG, Berlin, Germany) as a bolus was injected intravenously at a velocity of 2 mL/s, followed by 25-cc saline flush using an automatic injector. After administration of contrast media, 6 phases of dynamic enhanced images were acquired at 55.4 seconds (axial), 110.8 seconds (axial), 146 seconds (sagittal), 221.6 seconds (axial), 292 s (sagittal), and 438 seconds (axial), respectively. Dynamic axial and sagittal MR parameters were as follows: TR/TE, 4.42/2.17; flip angle, 12 degrees; field of view, 320 mm; matrix, 320/320; receiver bandwidth, 621.4 Hz/pixel; and slice thickness, 1 mm and 4.37/2.15; 12 degrees; 25 cm; 250/250; 704.5 Hz/pixel; 1 mm, respectively. Subtraction images were obtained by subtracting the pre-contrast images from the series of 6 postcontrast images on a pixel-by-pixel basis.

2.7. DCE-MRI and DWI analysis

Precontrast and DCE-MRIs were transferred to a commercially available MR computer-aided diagnosis workstation (CAD STREAM version 5.2.8.591, Confirma, Kirkland, WA) and were retrospectively reviewed. The kinetic analyses for breast lesions were reviewed by a radiologist (JC with 10 years of experience in breast imaging) blinded to clinical information and final histopathologic results. A color overlay map was placed on all enhancing lesions at a 50% enhancement threshold level in a pixel-by-pixel comparison across precontrast, first postcontrast, and last postcontrast series. The delayed enhancement type after the first postcontrast series was categorized as persistent, plateau, or washout pattern according to the changes of signal intensity after reaching the highest value.

Angio volume (cc) of the primary breast lesion, which represents total enhancing lesion volume, was measured automatically using CAD software. The quantitative parameters from kinetic curves were investigated including the proportion (%) of washout and plateau patterns. The percentage of peak enhancement in breast tumor lesions, which was defined as the peak value of the signal intensity, was also recorded using the following formula: (peak of signal intensity − signal intensity of precontrast phase)/signal intensity of precontrast phase × 100.

All DWIs were analyzed to measure the apparent diffusion coefficient (ADC) value ($\times 10^{-6}$ mm^2/s) by the same radiologist, who manually drew the ROI with care to avoid cystic and necrotic portions of the tumor and normal breast parenchyma. The ADC value was estimated using the following equation: $-(1/b)\ln(S_0/S_1)$, where b is the diffusion factor, S_1 is the attenuated signal (b value of 1000 s/mm^2) and S_0 is the full spin-echo signal without diffusion gradient (b value of 0 s/mm^2). Three ROIs were initially drawn on the most representative image corresponding to tumor location and size, after that the average ADC (ADC_{avg}) value was used for further analysis. Consensus was achieved in all patients.

2.8. Statistical analysis

All data are presented as mean ± standard deviation (SD) and the 95% confidence interval (CI). Statistical analysis was performed using the MedCalc software package (Ver. 9.5, MedCalc Software, Mariakerke, Belgium). Receiver operating characteristic (ROC) analysis was performed to estimate optimal cutoff values for all continuous variables for the prediction of disease recurrence. The Kaplan–Meier method with a log-rank test was assessed in univariate analyses of RFS using optimal cutoff values. Prognostic factors that were statistically significant in the Kaplan–Meier analysis were included in the multivariate analysis using Cox proportional hazard modeling to demonstrate independent prognostic factors for RFS. Statistical significance was defined as a $P < .05$.

3. Results

3.1. Patient characteristics and clinicohistologic features

Table 1 shows the patient characteristics. Disease recurrence occurred in 18 patients during the follow-up period (mean period 36.1 ± 13.6 months; range, 6.1–70.4 months). Of these patients, 5 showed locoregional recurrence, 4 experienced pulmonary metastasis, 3 had axillary lymph nodal metastasis, and 2 each had bone, brain, and liver metastases, respectively.

Table 2 includes the univariate analyses of the correlation between clinicohistologic features and RFS. Patients with pT diameter greater than 3 cm ($P < .001$) and higher pN stage ($P < .001$) showed poorer prognosis compared to those without. Higher nuclear and histologic grade was also significantly associated with poor prognosis ($P = .006$ and .006). Negative ER ($P = .005$), negative PR ($P = .044$), and positive Her-2 ($P = .049$) status were predictive of poor prognosis, but age ($P = .955$) and Ki67 overexpression ($P = .189$) were not. Figure 1 contains Kaplan-Meier curves according to clinicohistologic features.

3.2. Imaging parameters and recurrence-free survival

Table 3 lists the results of univariate analyses of DTP PET/CT parameters and RFS according to the optimal cutoff values from ROC curves. Patients with higher values of SUV_{max} ($P = .012$), MTV ($P < .001$), TLG ($P < .001$), SUV_{ALN} ($P < .001$), $\%\Delta SUV_{max}$ ($P < .001$), and $\%\Delta SUV_{ALN}$ ($P = .008$) had significantly lower RFS than those with lower values for those parameters. In addition, patients with a lower %ΔMTV value ($P = .002$) had a poor prognosis compared with those with a high value. There was no significant difference in RFS according to a cutoff value of %ΔTLG ($P = .431$). Kaplan-Meier curves for each group are illustrated in Fig. 2.

Univariate analyses of DCE-MRI and DWI parameters used to predict RFS are listed in Table 4. Kaplan–Meier curves revealed that only ADC_{avg} was significantly correlated with RFS ($P = .041$). Angio volume, proportion of washout pattern, proportion of plateau pattern, and peak enhancement were not associated with RFS ($P = .105$, .1460, .098, and .161, respectively). Kaplan–Meier curves of each group are illustrated in Fig. 3.

Table 1

Patient characteristics.

No. of patients		70
Age, y		
	Mean ± SD	50.5 ± 10.0
	Range	31–77
Follow-up period, mo	Mean ± SD	36.1 ± 13.6
	Range	6.1–70.4
Surgical treatment	BCS with ALND	49
	MRM with ALND	21
Adjuvant treatment	CTx + RTx + HTx	51
	CTx + RTx	9
	RTx + HTx	3
	CTx + HTx	3
	CTx only	4
pT stage	T1c	16
	T2	49
	T3	5
pN stage	N1	45
	N2	14
	N3	11
Disease group	Recurrence-free	52
	Recurrence	18

ALND = axillary lymph node dissection, BCS = breast conserving surgery, CTx = chemotherapy, HTx = hormone therapy, MRM = modified radical mastectomy, pN = pathologic lymph node, pT = pathologic tumor, RTx = radiotherapy, SD = standard deviation.

Table 2

Results of univariate analyses of clinicopathologic variables.

Variable		No. of recurrence	Mean survival, mo	*P*
Age, y	>50	9/34	37.1 ± 12.5	.955
	≤50	9/36	35.2 ± 14.5	
pT diameter, cm	>3	11/18	28.1 ± 13.8	<.001*
	≤3	7/52	38.9 ± 12.4	
pN stage	N1	6/45	39.1 ± 11.8	<.001*
	N2	5/14	34.5 ± 16.1	
	N3	7/11	26.0 ± 11.6	
Nuclear grade	NG1 + NG2	3/33	37.7 ± 11.6	.006*
	NG3	15/37	34.7 ± 15.1	
Histologic grade	HG1 + HG2	4/36	38.2 ± 11.1	.006*
	HG3	14/34	33.9 ± 15.5	
ER	Positive	9/52	38.2 ± 13.4	.005*
	Negative	9/18	30.0 ± 12.4	
PR	Positive	11/54	37.8 ± 13.8	.044*
	Negative	7/16	30.2 ± 11.4	
Her-2	Positive	9/21	34.4 ± 12.9	.049*
	Negative	9/49	36.8 ± 13.8	
Ki67 overexpression	Positive	15/50	34.2 ± 12.6	.189
	Negative	3/20	40.8 ± 14.9	

ER = estrogen receptor, Her-2 = human epidermal growth factor receptor 2, HG = histologic grade, NG = nuclear grade, pN = pathologic lymph node, PR = progesterone receptor, pT = pathologic tumor.
* $P < .05$.

3.3. Multivariate analysis

The multivariate regression analysis (Table 5), $\%\Delta SUV_{max}$ ($P = .043$) showed independent prognostic value along with ADC_{avg} ($P = .020$), ER status ($P = .002$), and pT diameter ($P = .001$). Figure 4 depicts a representative case.

4. Discussion

ALN status is the most significant prognostic factor and is considered in the application of adjuvant therapy after surgical treatment.[19] Postoperative adjuvant therapy can help eradicate cancer cells that might already have spread at the time of diagnosis. Even though adjuvant therapy improves survival, many patients still remain at risk of disease recurrence.[20] Therefore, we proposed that it would be clinically effective to identify breast cancer patients with metastatic ALN at higher risk of disease recurrence based on quantitative imaging parameters during preoperative evaluation. Although DCE-MRI and DWI are valuable imaging techniques for improving the sensitivity and specificity of malignant breast lesion detection, the prognostic significance of parameters derived from them compared with DTP PET/CT parameters has not been evaluated.

Our major finding was that only the percentage change in SUV_{max} during interval image acquisition time was an independent prognostic factor, along with ADC_{avg}, pT diameter, and ER status for RFS in IDC with metastatic ALN. According to the results of our multivariate analysis, both pT diameter and ER status were stronger prognostic markers than the 2 imaging parameters. Given that these clinicohistologic variables are obtained from surgical specimens, they might be expected to have greater prognostic value. However, in light of the ability to

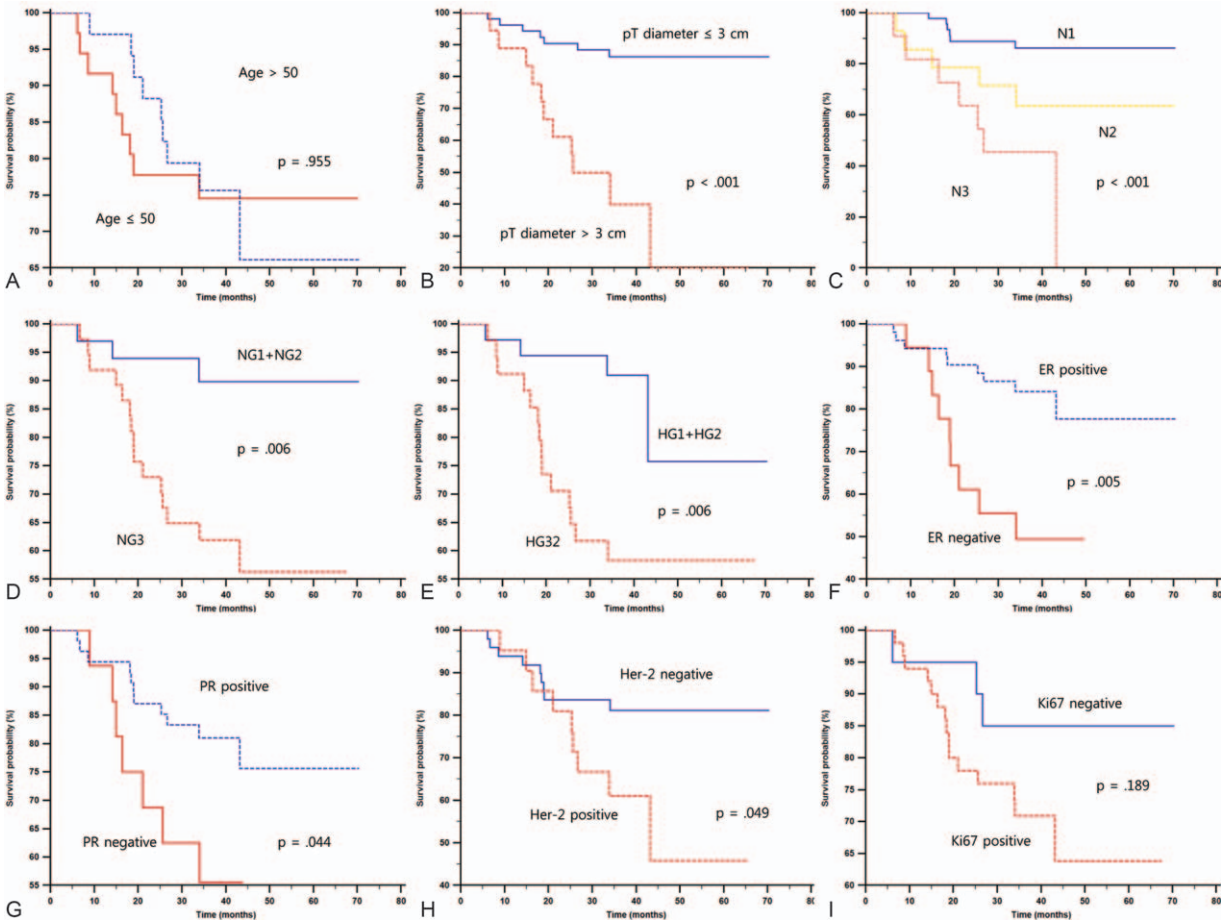

Figure 1. Kaplan–Meier curves of RFS for clinicohistologic variables: (A) Age, (B) pT diameter, (C) pN stage, (D) nuclear grade, (E) histologic grade, (F) ER status, (G) PR status, (H) Her-2 status, and (I) Ki67 overexpression. ER = estrogen receptor, pN = pathologic lymph node, RFS = recurrence-free survival.

evaluate prognosis using imaging parameters in a preoperative assessment, our results will have clinical implications. Our current findings are consistent with previously reported results from Garcia et al,[21] who suggested that the ^{18}F-FDG retention index showed prognostic value, and Choi et al,[22] who demonstrated that both SUV_{max} at a single time point and ADC values could be useful for predicting IDC prognosis. However, these prior studies did not include DTP PET parameters for survival analysis.

Table 3

Results of univariate analysis of DTP PET/CT parameters.

Variable	Cutoff value	No. of recurrence	Mean survival (months)	*P*
SUV_{max}	>5.73	15/39	34.1±13.6	.012*
		3/31	38.7±13.3	
MTV	>6.36	10/17	33.9±19.6	<.001*
		8/53	36.8±11.0	
TLG	>23.70	12/22	34.2±18.3	<.001*
		6/48	37.0±10.7	
SUV_{ALN}	>2.29	14/31	32.4±15.5	<.001*
		4/39	39.1±11.1	
$\%\Delta SUV_{max}$	>25.05	10/18	33.1±20.8	<.001*
		8/52	37.2±9.8	
%ΔMTV	≤−16.88	15/37	33.3±16.4	.002*
		3/33	39.3±8.6	
%ΔTLG	>−2.01	10/32	35.8±13.1	.431
		8/38	36.3±14.0	
$\%\Delta SUV_{ALN}$	>−0.40	17/47	35.3±15.8	.008*
		1/23	37.8±7.0	

DTP PET/CT = dual time point ^{18}F-fluorodeoxyglucose positron emission tomography/computed tomography, MTV = metabolic tumor volume, $SUV_{ALN} = SUV_{max}$ of axillary lymph node, SUV_{max} = maximal standardized uptake value, TLG = total lesion glycolysis.
* $P < .05$.

Based on this hypothesis, increasing SUV_{max} during the interval time would indicate the cancer cell aggressiveness. Univariate survival analyses revealed that both SUV_{max} and $\%\Delta SUV_{max}$ of the primary tumor had statistical value, whereas the multivariate analysis demonstrated that only $\%\Delta SUV_{max}$ was an independent prognostic factor. SUV_{max} only represents the highest radiotracer concentration at a single time point, and so the percentage change in FDG accumulation would be expected to reflect metabolic characteristics of breast cancer better than a static parameter.

The quantitative DCE-MRI parameters from the CAD program that predominantly depend on microvascular permeability and blood flow rate did not provide prognostic information for risk stratification in this study. However, our results differ from those of Pickles et al,[23] who asked whether DCE-MRI vascular kinetic variables and MRI-based volume had a prognostic value in locally advanced breast cancer patients. This dissimilarity may be related to the different methods of imaging analysis to obtain tumor size, vascular kinetic parameters, texture, and shape-based metrics.

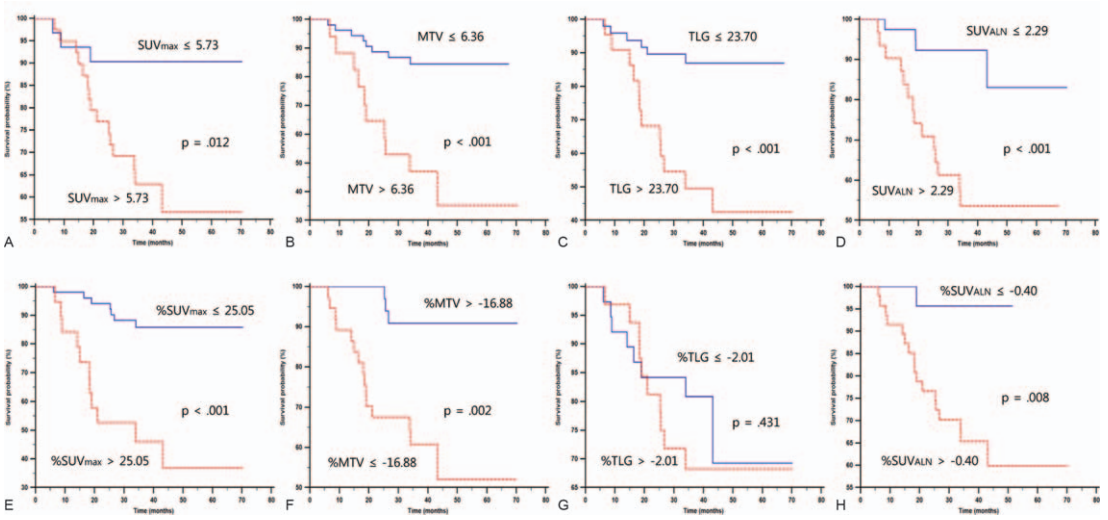

Figure 2. Kaplan–Meier curves of RFS for subgroups according to DTP PET/CT parameters: (A) SUV_{max}, (B) MTV, (C) TLG, (D) SUV_{ALN}, (E) $\%\Delta SUV_{max}$, (F) %ΔMTV, (G) %ΔTLG, and (H) $\%\Delta SUV_{ALN}$. DTP = dual time point, ER = estrogen receptor, MTV = metabolic tumor volume, PET/CT = positron emission tomography/computed tomography, RFS = recurrence-free survival, SUV = standardized uptake value, TLG = total lesion glycolysis.

Table 4

Results of univariate analysis of DCE-MRI and DWI parameters.

Variable	Cutoff value	No. of recurrence	Mean survival (mons)	*P*
Angio volume, cc	>15.1	5/11	33.0±12.9	.105
		13/59	36.7±13.7	
Proportion of washout pattern, %	>1.1	17/58	35.2±13.7	.146
		1/12	40.7±12.5	
Proportion of plateau pattern, %	>17.3	14/44	32.9±12.2	.098
		4/26	41.5±14.2	
Peak enhancement, %	≤341.2	15/48	36.3±15.7	.161
		3/22	35.7±7.4	
ADC_{avg}, $\times 10^{-6}\,mm^2/s$)	≤1016.55	12/32	34.3±15.7	.041*
		6/38	37.6±11.4	

ADC_{avg} = average apparent diffusion coefficient, DCE-MRI = dynamic contrast enhanced magnetic resonance imaging, DWI = diffusion weighted imaging.
* $P < .05$.

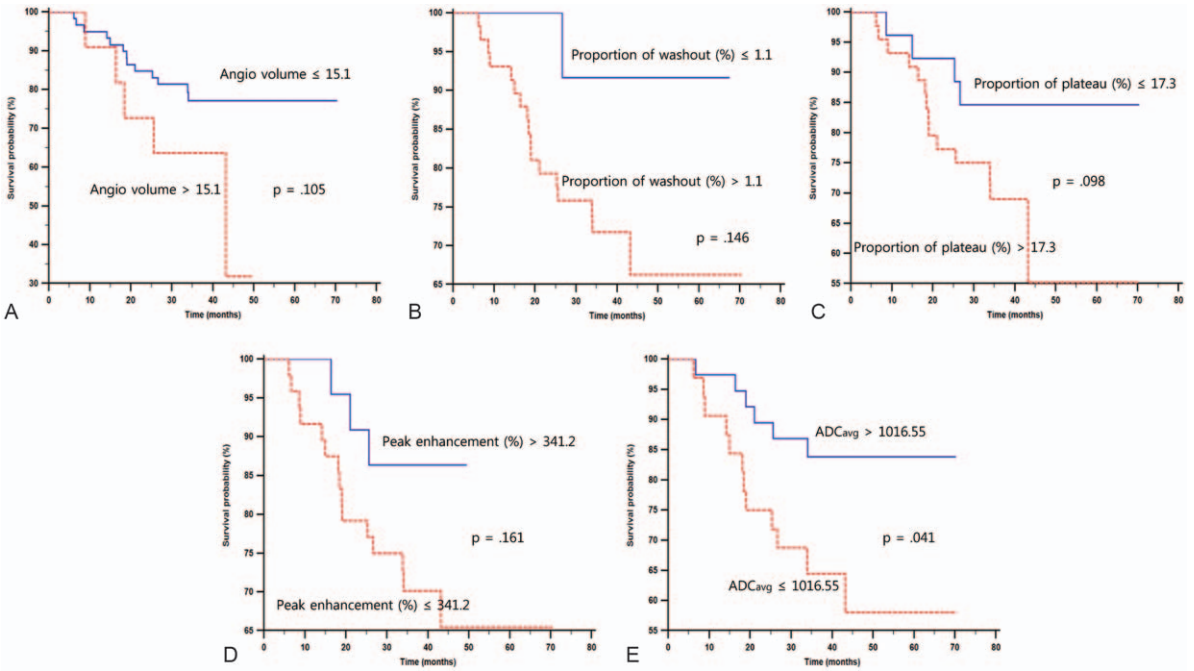

Figure 3. Kaplan-Meier curves of RFS for subgroups according to DCE-MRI and DWI parameters: (A) Angio volume (cc), (B) proportion of washout (%), (C) proportion of plateau (%), (D) peak enhancement (%), and (E) ADC_{avg} ($\times 10^{-6}\,mm^2/s$). ADC = apparent diffusion coefficient, DCE-MRI = dynamic contrast enhanced magnetic resonance imaging, DWI = diffusion-weighted imaging, ER = estrogen receptor, RFS = recurrence-free survival.

Table 5

Results of multivariate analysis for RFS.

Variable	HR	95% CI	P
ER negativity	5.3902	1.8315–15.8634	.002*
pT diameter (cm) >3	5.4047	1.9433–15.0315	.001*
ADC_{avg} ($\times 10^{-6} mm^2/s$) ≤1016.55	3.9565	1.2506–12.5175	.020*
$\%\Delta SUV_{max}$ >25.05	2.9287	1.0397–8.2499	.043*

ADC_{avg} = average apparent diffusion coefficient, CI = confidence interval, ER = estrogen receptor, HR = hazard ratio, pT = pathologic tumor, RFS = recurrence-free survival, SUV_{max} = maximal standardized uptake value.

* $P < .05$.

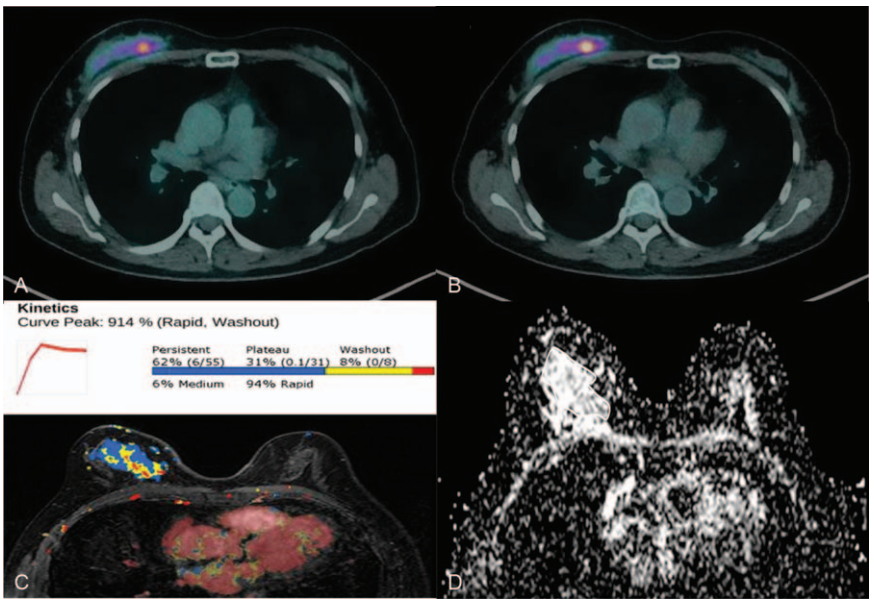

Figure 4. A 56-year-old patient with IDC in the upper outer quadrant of the right breast and metastatic ALN: $\%\Delta SUV_{max}$, 25.25, ADC_{avg}, $925.36 \times 10^{-6} mm^2/s$, pT diameter, 3.2 cm, negative ER: (A) early-phase fusion PET/CT, (B) delayed-phase fusion PET/CT, (C) DCE MRI with the kinetic curve, and (D) ADC map showing ROI for measuring the ADC_{avg}. The patient experienced recurrence in the right chest wall after 17.8 months. ADC = apparent diffusion coefficient, ALN = axillary lymph node, ER = estrogen receptor, IDC = invasive ductal breast cancer, ROI = region of interest, SUV = standardized uptake value.

This study has several limitations. First, the exclusive focus on ALN-positive patients might limit the generalizability of our results. Second, given the limited resolution of PET (e.g., partial volume effect), the SUV_{max} of either small primary tumor lesions (e.g., smaller than 2 cm) or ALN could be underestimated.[24] However, the partial volume effect should be negligible in this study because there were no patients with disease recurrence in the T1c group and only 1 patient with an SUV_{ALN} lower than 1 had disease recurrence during follow-up. Third, we did not analyze the morphologic characteristics of breast lesions such as tumor shape, tumor margin or contrast-enhancement patterns using DCE-MRI, which may be associated with histopathologic grade.[25,26] Therefore, further prospective studies that complement our approach and evaluate the specific criteria of morphologic characteristics to determine prognosis are necessary in the future.

Despite these limitations, the current study demonstrated that quantitative imaging parameters using DTP PET/CT and DWI had independent prognostic significance for patients with ALN-positive IDC. As breast cancer patients with metastatic ALN have poorer prognoses than those without, further classification of this patient group according to objective prognostic factors during preoperative clinical assessment would be valuable for optimizing treatment approach. The prognostic value of those imaging parameters can be evaluated to provide evidence for risk stratification, guiding the treatment plan for individual patients and ultimately improving prognosis.

References

[1] Love C, Tomas MB, Tronco GG, et al. FDG PET of infection and inflammation. Radiographics 2005;25:1357–68.
[2] Metser U, Even-Sapir E. Increased (18)F-fluorodeoxyglucose uptake in benign, nonphysiologic lesions found on whole-body positron emission tomography/computed tomography (PET/CT): accumulated data from four years of experience with PET/CT. Semin Nucl Med 2007;37:206–22.
[3] Houshmand S, Salavati A, Seqtnan EA, et al. Dual-time-point imaging and delayed-time-point fluorodeoxyglucose-PET/computed tomography imaging in various clinical settings. PET Clin 2016;11:65–84.
[4] Schillaci O. Use of dual-point fluorodeoxyglucose imaging to enhance sensitivity and specificity. Semin Nucl Med 2012;42:267–80.
[5] Petralia G, Bonello L, Priolo F, et al. Breast MR with special focus on DW-MRI and DCE-MRI. Cancer Imag 2011;11:76–90.
[6] Rahbar H, Partridge SC. Multiparametric MR imaging of breast cancer. Magn Reson Imaging Clin N Am 2016;24:223–38.
[7] Choi SY, Chang YW, Park HJ, et al. Correlation of the apparent diffusion coefficiency values on diffusion-weighted imaging with prognostic factors for breast cancer. Br J Radiol 2012;85:e474–9.

[8] El Khouli RH, Macura KJ, Jacobs MA, et al. Dynamic contrast-enhanced MRI of the breast: quantitative method for kinetic curve type assessment. Am J Roentgenol 2009;193:W295–300.
[9] Razek AA, Gaballa G, Denewer A, et al. Invasive ductal carcinoma: correlation of apparent diffusion coefficient value with pathological prognostic factors. NMR Biomed 2010;23:619–23.
[10] de Boer M, van Dijck JA, Bult P, et al. Breast cancer prognosis and occult lymph node metastases, isolated tumor cells, and micrometastases. J Natl Cancer Inst 2010;102:410–25.
[11] Schiffman SC, McMasters KM, Scoggins CR, et al. Lymph node ratio: a proposed refinement of current axillary staging in breast cancer patients. J Am Coll Surg 2011;213:45–52.
[12] Boellaard R, O'Doherty MJ, Weber WA, et al. FDG PET and PET/CT: EANM procedure guidelines for tumour PET imaging: version 1.0. Eur J Nucl Med Mol Imaging 2010;37:181–200.
[13] Kaida H, Toh U, Hayakawa M, et al. The relationship between 18F-FDG metabolic volumetric parameters and clinicopathological factors of breast cancer. Nucl Med Commun 2013;34:562–70.
[14] Collins LC, Botero ML, Schnitt SJ. Bimodal frequency distribution of estrogen receptor immunohistochemical staining results in breast cancer: an analysis of 825 cases. Am J Clin Pathol 2005;123:16–20.
[15] Wolff AC, Hammond ME, Schwartz JN, et al. American Society of Clinical Oncology/College of American Pathologists guideline recommendations for human epidermal growth factor receptor 2 testing in breast cancer. J Clin Oncol 2007;25:118–45.
[16] Cheang MC, Chia SK, Voduc D, et al. Ki67 index, HER2 status, and prognosis of patients with luminal B breast cancer. J Natl Cancer Inst 2009;101:736–50.
[17] Chen LY, Tsang JY, Ni YB, et al. Bcl2 and Ki67 refine prognostication in luminal breast cancers. Breast Cancer Res Treat 2015;149:631–43.
[18] Lee JW, Cho A, Lee JH, et al. The role of metabolic tumor volume and total lesion glycolysis on (1)(8)F-FDG PET/CT in the prognosis of epithelial ovarian cancer. Eur J Nucl Med Mol Imaging 2014;41: 1898–906.
[19] Cianfrocca M, Goldstein LJ. Prognostic and predictive factors in early-stage breast cancer. Oncologist 2004;9:606–16.
[20] Jemal A, Siegel R, Xu J, et al. Cancer statistics, 2010. CA Cancer J Clin 2010;60:277–300.
[21] Garcia Vicente AM, Castrejon AS, Relea Calatayud F, et al. 18F-FDG retention index and biologic prognostic parameters in breast cancer. Clin Nucl Med 2012;37:460–6.
[22] Choi BB, Kim SH, Kang BJ, et al. Diffusion-weighted imaging and FDG PET/CT: predicting the prognoses with apparent diffusion coefficient values and maximum standardized uptake values in patients with invasive ductal carcinoma. World J Surg Oncol 2012;10:126.
[23] Pickles MD, Lowry M, Gibbs P. Pretreatment prognostic value of dynamic contrast enhanced magnetic resonance imaging vascular, texture, shape, and size parameters compared with traditional survival indicators obtained from locally advanced breast cancer patients. Invest Radiol 2016;51:177–85.
[24] Soret M, Bacharach SL, Buvat I. Partial-volume effect in PET tumor imaging. J Nucl Med 2007;48:932–45.
[25] Lee SH, Cho N, Kim SJ, et al. Correlation between high resolution dynamic MR features and prognostic factors in breast cancer. Korean J Radiol 2008;9:10–8.
[26] Huang J, Yu J, Peng Y. Association between dynamic contrast enhanced MRI imaging features and WHO histopathological grade in patients with invasive ductal breast cancer. Oncol Lett 2016;11: 3522–6.